



Dynamics of the artificially created vacancies in the monomolecular C₆₀ layers



D.A. Olyanich^{a,b}, T.V. Utas^{a,b}, A.V. Zotov^{a,b,c,*}, A.A. Saranin^{a,b}

^a Institute of Automation and Control Processes, 5 Radio Street, 690041 Vladivostok, Russia

^b School of Natural Sciences, Far Eastern Federal University, 690950 Vladivostok, Russia

^c Department of Electronics, Vladivostok State University of Economics and Service, 690600 Vladivostok, Russia

ARTICLE INFO

Article history:

Received 28 December 2014

Accepted 20 February 2015

Available online 28 February 2015

Keywords:

Atom–solid interactions

Silicon

Fullerene

Self-assembly

Scanning tunneling microscopy

ABSTRACT

Dynamics of single and double vacancies within the monomolecular C₆₀ layer on the In-modified Au/Si(111) $\sqrt{3} \times \sqrt{3}$ surface have been studied by means of variable temperature scanning tunneling microscopy (STM). The vacancies were deliberately created in the layer using STM tip impact in the regimes below decomposition threshold. Single vacancy motion has been found to be a thermally activated process characterized by the activation energy of 1.5 ± 0.3 eV. This is an effective activation energy which agrees with the net value consisted of the term responsible for vacancy migration within the free-standing C₆₀ layer, 0.88 eV and that for individual C₆₀ migration on (Au, In)/Si(111) surface, -0.4 eV. Mobility of C₆₀ vacancies has been found to be affected by In adatoms. It can be slowed down by more than an order of magnitude by deposition of only 0.2 monolayer of additional In. The double vacancies have been found to be more mobile than single vacancies in which its effect is provided by a specific rotational mechanism of their motion.

© 2015 Elsevier B.V. All rights reserved.

1. Introduction

Manipulation of molecules using scanning tunneling microscopy (STM) is a promising technique for creating molecular nanostructures with desired geometry and properties. Manipulation of molecules, such as C₆₀ fullerenes has been successfully performed on metal and semiconductor surfaces [1,2]. The most work in this field has so far been devoted to manipulation of isolated single fullerenes using their pushing, pulling and sliding by an STM tip [3–12]. The obtained results demonstrate a principal possibility for fabricating nanostructures by moving fullerenes one by one into the desired positions on the surface. Alternative approach for nanostructure formation resides in taking a continuous monomolecular layer or array, selecting “excess” fullerenes and by their removal getting a desired molecular nanostructure. It has been demonstrated that this can be done by decomposition of the selected C₆₀ molecules by heating them using electron current passing through the tip–molecule junction [13,14]. However, this technique might have undesirable side effects, such as destruction of the substrate and contamination of the surface by fragments of the decomposed fullerenes. Very recently, we have demonstrated that in the mild regimes, below decomposition threshold, one can manipulate the pre-selected C₆₀ in the molecular layer using purely mechanical impact of the STM

tip on C₆₀ molecule [15]. Combination of knockout of the chosen C₆₀ (i.e., vacancy formation) and shifting of the C₆₀ molecule to the neighboring vacant site (if available) allows formation of the desired vacancy pattern. As an example, Fig. 1 shows a regular hexagonal pattern of artificially created vacancies built in this manner. For the STM movie illustrating the fabrication process one can address the Supplemental material (Part 1) [16].

Having developed such a method for fabricating vacancy patterns, we have pursued two goals by performing the present study. The first can be thought as an applied task to determine the range of thermal stability of the created vacancy patterns. The second is a scientific problem of elucidating mechanisms controlling mobility of the vacancies within monomolecular C₆₀ layer. It is worth saying that vacancy dynamics can play an important role in many surface phenomena like surface diffusion, thin film growth, step motion or catalysis. Though STM seems to be an ideal tool for studying vacancies on the atomic scale, we are aware of only two researches [17,18] where vacancy dynamics was studied by direct monitoring of the displacements of single atomic vacancies. To our knowledge, our work is the first one where a similar study has been performed for vacancies in the monomolecular layer.

In the present paper, we reported on the results of the STM study of the diffusion of single vacancies artificially created with an STM tip in the C₆₀ monomolecular layers grown on In-modified Au/Si(111) $\sqrt{3} \times \sqrt{3}$ surface. The diffusion barrier for single vacancy migration has been determined to be 1.5 ± 0.3 eV. It has been found that presence of a small amount of mobile In atoms at the surface retards the vacancy

* Corresponding author at: Institute of Automation and Control Processes, 5 Radio Street, 690041 Vladivostok, Russia.

E-mail address: zotov@iacp.dvo.ru (A.V. Zotov).

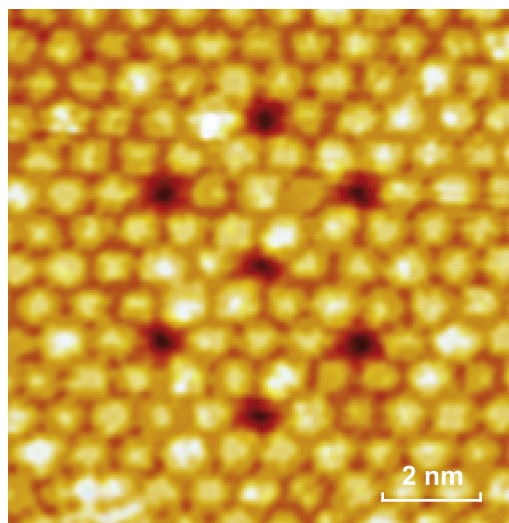


Fig. 1. Hexagonal vacancy pattern created in the C_{60} monomolecular layer using STM manipulations in the regime below the decomposition threshold.

motion which can be slowed down by more than an order of magnitude by depositing additional In. The double vacancies have been found to be more mobile than single vacancies due to the rotational mechanism of their motion with lowered diffusion barriers.

2. Experimental details

Our experiments were performed with a variable-temperature Omicron VT-STM operating in an ultrahigh vacuum ($\sim 2.0 \times 10^{-10}$ Torr). Atomically-clean Si(111) 7×7 surfaces were prepared in situ by flashing to 1280 °C after the samples were first outgassed at 600 °C for several hours. Gold was deposited from an Au-wrapped tungsten filament, indium from Ta crucible and C_{60} fullerenes from a resistively heated Mo crucible. To prepare the In-modified Au/Si(111) $\sqrt{3} \times \sqrt{3}$ surface, the Au/Si(111) $\sqrt{3} \times \sqrt{3}$ surface [19] was first formed by Au deposition onto Si(111) 7×7 surface held at 700 °C and then ~ 0.5 ML of In was deposited onto this surface held at room temperature followed by brief (~ 15 s) annealing at 600 °C. The resultant surface was highly-ordered and homogeneous being free of domain walls, characteristic of the pristine Si(111) $\sqrt{3} \times \sqrt{3}$ -Au surface. It preserves the atomic arrangement of the $\sqrt{3} \times \sqrt{3}$ -Au phase and contains ~ 0.15 ML of In left after high-temperature treatment and forming a 2D gas of mobile adatoms [20,21].

Room-temperature deposition of C_{60} onto this surface results in the formation of the close-packed hexagonal C_{60} molecular arrays which periodicity coincides with the bulk fullerite nearest-neighbor distance of 10.02 Å [22]. Two types of C_{60} arrays with different orientations form. In the arrays of the first type (0° -rotated arrays), the molecular rows are aligned along the principal crystallographic directions of the Si(111) surface, i.e., $\langle 10\bar{1} \rangle$. These arrays display a characteristic Moiré pattern of dim and bright C_{60} fullerenes which indicates the difference in their adsorption geometries and energies [23]. In the arrays of the second type (19.1° -rotated arrays), the molecular rows make an angle of $\pm 19.1^\circ$ with the $\langle 10\bar{1} \rangle$ directions. In the 19.1° -rotated arrays, all fullerenes exhibit the same STM contrast which can be treated as a sign of a similar bonding state. In the present work the vacancy motion only in the 19.1° -rotated arrays was studied to facilitate analysis of the obtained data.

For STM observations and C_{60} manipulations, electrochemically etched tungsten tips cleaned by in situ heating were employed. To produce a vacancy in the C_{60} molecular monolayer, we used a ‘z-pulse’ technique [13,14] as follows. First, STM image of the C_{60} array was

acquired using normal tunneling conditions (e.g., at -1.5 V and 0.3 nA). Then, STM tip was placed above a chosen C_{60} , the feedback was switched off, the desired sample bias voltage V_s and current were preset, and the tip approached a distance Z towards a C_{60} and retreated back holding V_s constant. During tip approach and retreat, the current flowing through the molecular junction could be recorded as a function of tip displacement, $I(Z)$. The result of manipulation was checked at subsequent STM observations at normal conditions. Extracted C_{60} fullerene becomes an ad-molecule on top of C_{60} layer and migrates away. Though ad-molecules cannot be detected by STM due to their extremely high mobility but their presence is manifested by occasional healing of some vacancies (i.e., filling of a vacancy by an ad-molecule) during STM observations. After creating the vacancies, the sample was kept at a fixed temperature for a prolonged time (typically, on the order of half to 2 h) during which the same surface region with vacancies was probed with STM. A set of successive STM images constitutes a data set to evaluate vacancy dynamics at a given temperature. As a final remark, we would like to note that STM observations at modest tunneling conditions used in the experiments produce no noticeable tip-induced effects on vacancy migration. All manipulations of C_{60} molecules on the surface are achieved only with direct mechanical impact of STM tip on a given fullerene. This concerns also shifting C_{60} to the neighboring vacant site within C_{60} monolayer (i.e., shifting a vacancy), as was considered in detail in Ref. [15].

3. Results and discussion

3.1. Single-vacancy dynamics

Fig. 2 illustrates experimental procedure used to evaluate mobility of the molecular vacancies in the C_{60} array using STM observations. In the shown area six vacancies were created which initial locations are indicated by open white circles. The trajectories of the vacancies after keeping the sample at 361 K for 38 min are highlighted by white lines (for the complete STM video see Supplemental material (Part 2) [16]). One can see that the vacancies are mobile at this temperature and commit many hops for the time of successive STM image acquisition, ~ 80 s.

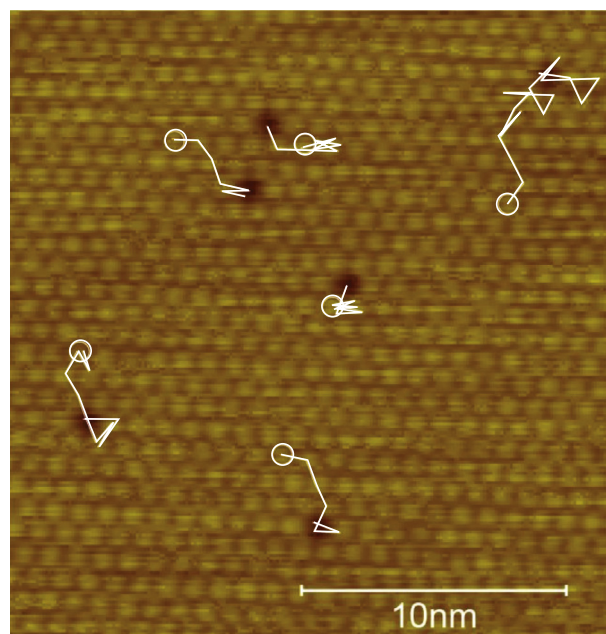


Fig. 2. STM image of the C_{60} layer region with six artificially created vacancies. The vacancy trajectories completed after keeping the sample at 361 K for 38 min are shown by the white lines with open circles indicating initial location of the vacancies. For complete STM video see Supplemental material (Part 2) [16].

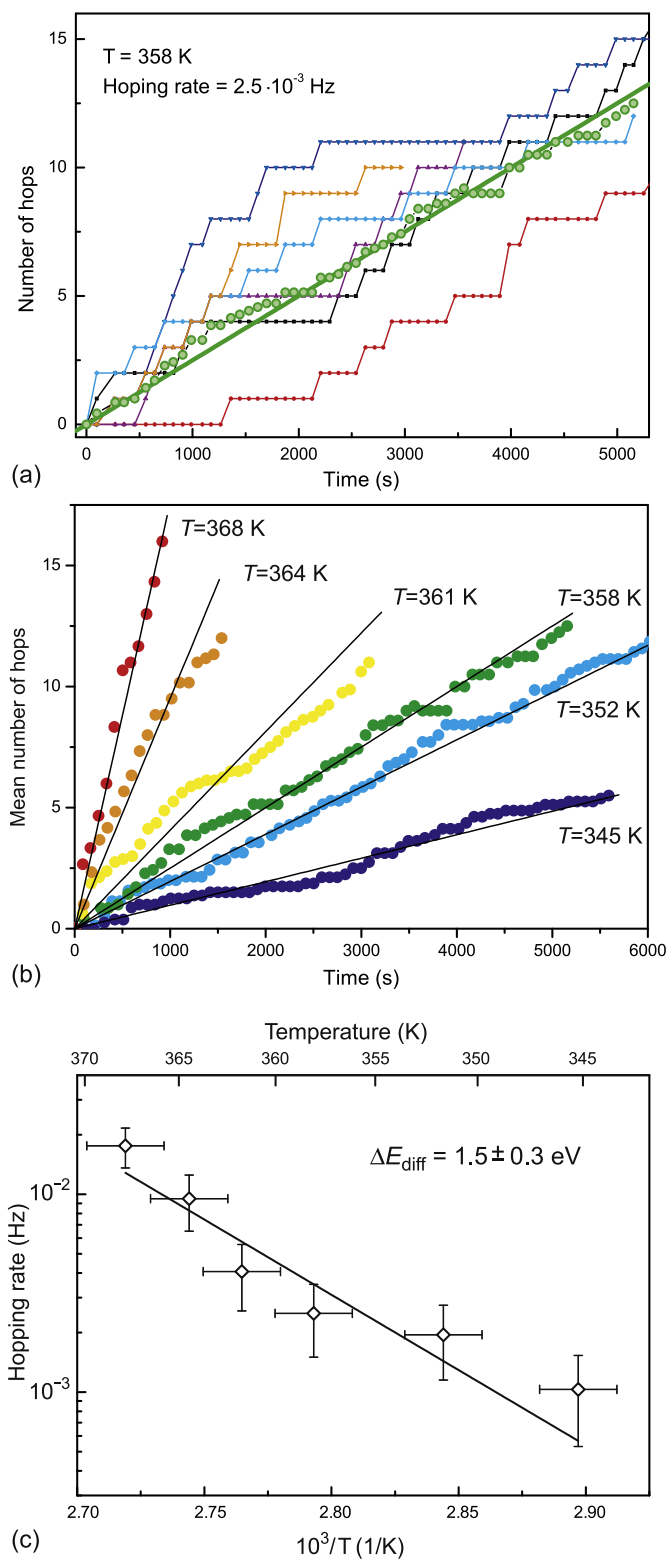


Fig. 3. (a) Number of hops committed by vacancies at 358 K during the period of about 85 min. Dependencies for each of six vacancies under consideration are shown by small circles of different colors. The mean dependence averaged over all vacancies is shown by large green circles. The linear fit for the dependence yields a mean hopping rate of $2.5 \times 10^{-3}\text{ Hz}$. (b) Mean dependencies obtained at six different temperatures (as indicated) combined into one graph. (c) Arrhenius plot of the vacancy hopping rate. (For interpretation of the references to color in this figure legend, the reader is referred to the web version of this article.)

However, it is worth noting that STM observations were conducted at relatively low temperatures which allow detecting almost every elemental (one-lattice-spacing long) hop. This fact justifies the use of hopping rates for evaluating a vacancy dynamics.

In quantitative characterizations of vacancy dynamics, about ten artificially created vacancies were monitored at each temperature through counting the number of elemental hops committed by vacancies during the observation period. From these data the mean hopping rate of a vacancy at a given temperature was extracted (Fig. 3a and b). The results obtained for the temperature interval from 345 to 368 K are summarized in the Arrhenius plot in Fig. 3c. The slope of the plot yields an activation barrier for vacancy diffusion of $1.5 \pm 0.3\text{ eV}$.

3.2. Simulation of vacancy migration

To add understanding of the vacancy migration mechanisms, we simulated vacancy motion in the closed packed C_{60} array where intermolecular C_{60} – C_{60} interaction was described by the pair interaction energy $E(r)$ calculated in [23] and approximated by the Buckingham potential (Fig. 4a). The energy of a given C_{60} molecule in the molecular array is defined as a sum of pair C_{60} – C_{60} interactions of a given fullerene with each of C_{60} molecules constituting the array. In turn, the energy of the array is defined as a sum of energies of all fullerenes excluding double counting. To find the local energy minimum of the array, the following procedure was employed. In each of the equidistant 360 points at a circle of radius 0.01 Å drawn from the center of a given fullerene, the potential produced by all other fullerenes was calculated. Then, the fullerene was moved to the point with the minimal potential. The

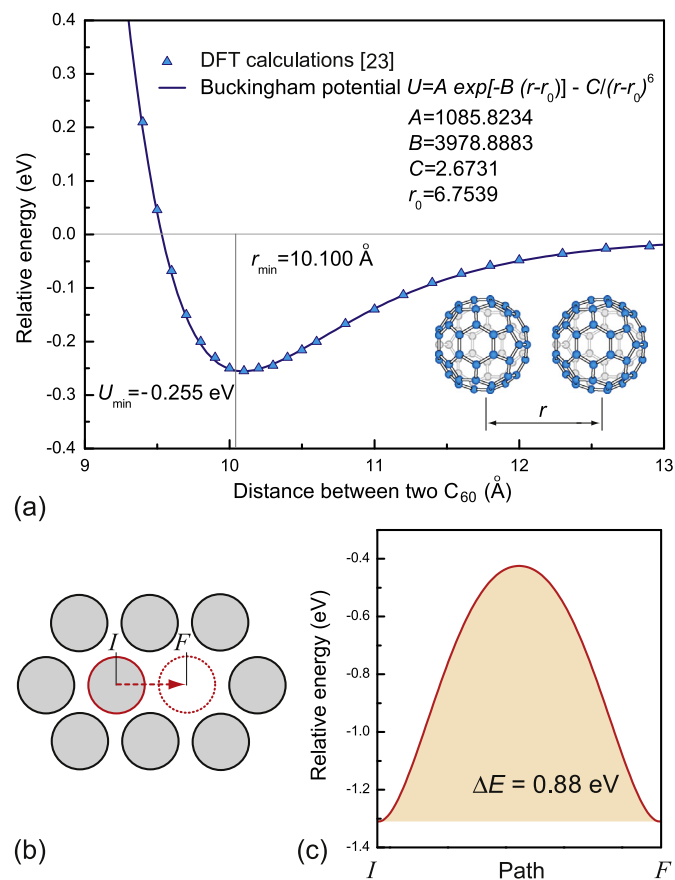


Fig. 4. Simulation of a single vacancy migration within the free-standing C_{60} monomolecular layer. (a) C_{60} – C_{60} pair interaction energy calculated in [23] and approximated by the Buckingham potential with the indicated parameters. (b) Diffusion path of fullerene from the initial location (indicated as I) to the final location (indicated as F) and (c) the calculated shape of the energy barrier along the I–F path.

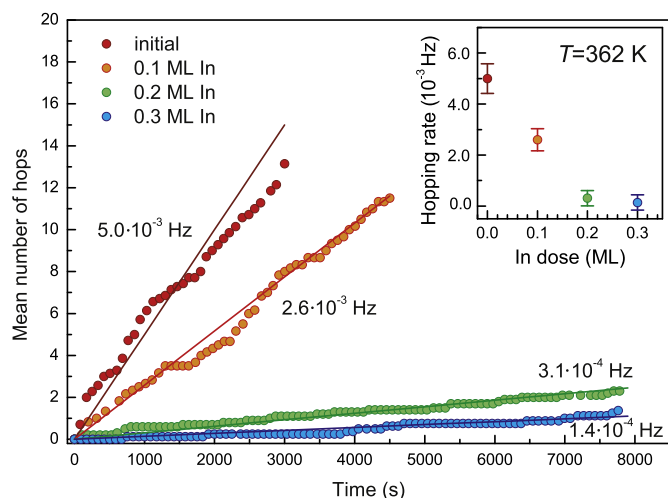


Fig. 5. (a) Mean number of hops executed by vacancies versus time for the original $C_{60}/(\text{Au}, \text{In})/\text{Si}(111)$ sample (red circles) and for those after depositing additional 0.1 ML (orange circles), 0.2 ML (green circles) and 0.3 ML In (blue circles). Inset shows dependence of hopping rate on the dose of additional In. (For interpretation of the references to color in this figure legend, the reader is referred to the web version of this article.)

procedure was repeated for all fullerenes until they occupy the minimal-energy positions and, hence, did not move. To simulate a motion of a given fullerene, the direction of motion was defined by a 90° sector and the fullerene was moved to the minimal-energy point on the circle of radius 0.01 \AA within the sector. After moving the fullerene to a new point, its location was fixed and all other fullerenes in array were allowed to relax and occupy the minimal-energy positions. Then, a new step of fullerene motion was conducted according to above procedure. In the simulations the array consisting of 400 fullerenes was treated.

As illustrated in Fig. 4, the simulation demonstrates that the C_{60} fullerene within the molecular array surmounts the energy barrier of 0.88 eV when going to the neighboring vacant site. This barrier is associated with tearing off the bonds with five neighboring molecules to move to the intermediate position with a lower coordination (see Fig. 4b and Supplemental material (Part 3) [16]). Note that simulation concerns the case of the flat free-standing C_{60} monomolecular layer. In reality, the layer resides on the $(\text{Au}, \text{In})/\text{Si}(111)$ surface and the C_{60} has to surmount also the diffusion barriers associated with motion along this surface. In Ref. [24], we investigated diffusion of the individual C_{60} molecules on $(\text{Au}, \text{In})/\text{Si}(111)$ surface via analysis of C_{60} island number density and found that barrier of surface diffusion equals $\sim 0.4 \text{ eV}$ at temperatures above 150 K . Thus, the net barrier for vacancy migration

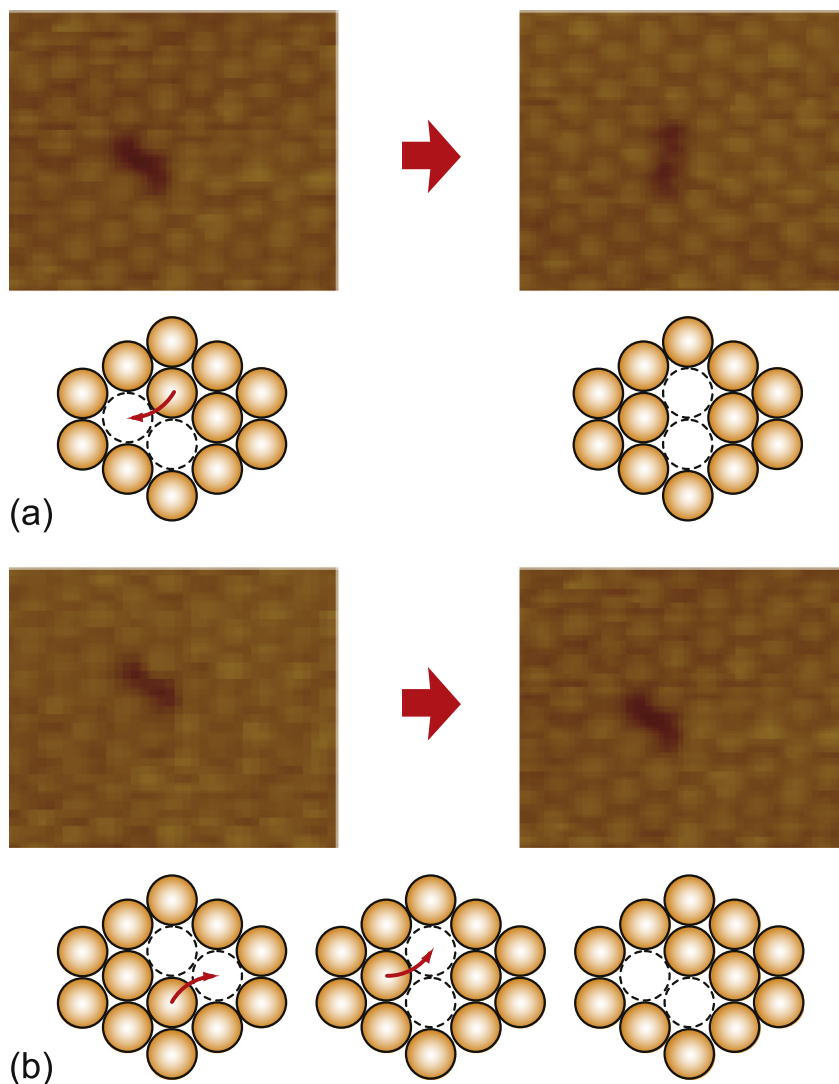


Fig. 6. Successive STM images and their schematics illustrating the rotational mechanism of double vacancy motion. (a) Elemental rotation step. (b) Two successive rotations resulting in an overall shift of a double vacancy.

within C_{60} monolayer on the In-adsorbed Au/Si(111) $\sqrt{3} \times \sqrt{3}$ surface can be estimated as a sum of two barriers, $0.88 + 0.4 \approx 1.3$ eV, which result in a reasonable agreement with the experimentally determined value, 1.5 ± 0.3 eV.

3.3. Effect of In adatoms on vacancy mobility

Let us consider the effect produced by surface In atoms on the molecular C_{60} vacancy migration in a greater detail. DFT calculations presented in Ref. [24] demonstrate that diffusion barrier for C_{60} migrating on the In-free Au/Si(111) surface is very low but it increases rapidly when C_{60} approaches the vicinity of the In adatom and C_{60} location atop In adatom is extremely energetically unfavorable. Therefore, one can expect that In adatoms can retard C_{60} vacancy migration in the molecular layer. This was, indeed, proved in the experiment with In deposition as illustrated in Fig. 5 (for STM videos see Supplemental material (Part 4) [16]). The data presented by red circles show the number of vacancy hops versus time for the C_{60} array on Au/Si(111) $\sqrt{3} \times \sqrt{3}$ surface containing usual In amount of ~ 0.15 ML. When additional 0.1 ML of In was deposited onto this surface, the dependence changes to the one shown by orange circles indicating almost halving of the vacancy hopping rate. After depositing 0.2 ML In, the hopping rate decreases by more than an order of magnitude. Vacancies become essentially immobile after dosing the sample with 0.3 ML In. It is worth noting that after In deposition no new features appear on the sample surface which can be attributed to the In 3D islands atop or beneath the C_{60} monolayer. Thus, it can be suggested that In penetrates through the C_{60} layer and increases the density of a 2D gas of mobile In adatoms on the substrate surface beneath the C_{60} layer.

We propose an explanation for the observed In-induced retardation of vacancy motion as being due to site blocking effect. Molecular vacancy can be temporarily occupied by In adatom (or adatoms) and probability of this event increases with increasing In coverage. When In atom resides in a vacancy, the neighboring C_{60} molecules have no chance to move to the vacancy position which represents then an energetically unfavorable site. The vacancy remains immobile until the moment when In adatom leaves the vacancy. As a result, the mean hopping rate of vacancies diminishes. The greater concentration of In adatoms on the surface the greater is the retardation of the vacancy motion.

3.4. Double-vacancy dynamics

As an addition task, we have considered the dynamics of double vacancies. The first main result of the observations is that a double vacancy demonstrates much higher mobility than a single vacancy. Double vacancies remain in motion even at room temperature (i.e., ~ 295 K) while single vacancies become essentially immobile already at ~ 340 K. Note that this behavior of vacancies contrasts to that of atoms or molecules on the surface where single species are frequently more mobile than their agglomerates. For example, it is a typical situation when critical cluster size $i = 1$ and dimer constitutes stable immobile cluster (e.g., as in case of the present system of C_{60} on the In-modified Au/Si(111) surface [24,25]). The next observation concerns the mechanism of double vacancy motion. Double vacancy rotation around one of the vacancies (see Fig. 6a) appears to be the most frequently observed type of their motion. Translational motion of double vacancy in forward direction (see Fig. 7a) has never been observed. However, the sideways shift of double vacancy (as illustrated by two successive STM images in

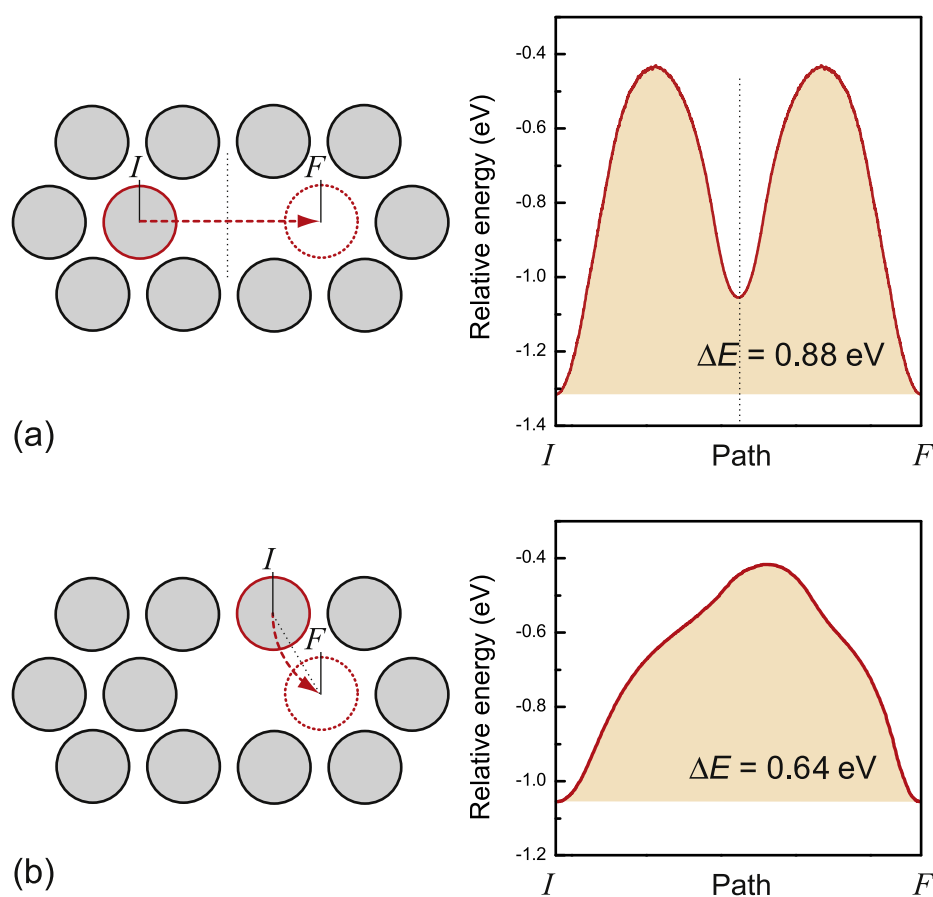


Fig. 7. Simulations of a double vacancy migration within the free-standing C_{60} monomolecular layer. (a) Diffusion I - F path and corresponding calculated shape of the energy barrier when a double vacancy moves via temporal decay into single vacancies. (b) The same as (a) but for the case of the double vacancy rotational motion.

Fig. 6b) is possible. However, such a motion can be thought also as a result of two successive rotations (see schematics in Fig. 6b).

Our simulations reproduce qualitatively the main results of STM observations. Fig. 7a demonstrates that translational motion of the double vacancy with its temporal decay into the two single vacancies is characterized by the barrier of 0.88 eV. One can see that this motion is essentially similar to the motion of a single vacancy, hence the same diffusion barrier. In the case of the rotational motion (Fig. 7b), a moving fullerene has in its starting point a lower number of the nearest neighbors, four instead of five as in the case of single-vacancy motion, and it moves along the optimal curved pass, hence the barrier is only 0.64 eV (i.e. 0.24 eV lower than that for a single vacancy motion). The barrier for sideways motion of double vacancy via simultaneous shifting two fullerenes is almost twice greater, therefore such an event has a very low probability.

4. Conclusion

In conclusion, we have deliberately created single and double vacancies in the monomolecular C₆₀ layer grown on the In-modified Au/Si(111) $\sqrt{3} \times \sqrt{3}$ surface and studied their dynamics using variable temperature STM observations. The activation energy of the single vacancy motion has been determined to be 1.5 ± 0.3 eV. The double vacancies are more mobile than single vacancies which is provided by the rotational mechanism of their motion. Specific feature of the C₆₀/(Au, In)/Si(111) system which has been found to produce unexpectedly great effect on the vacancy dynamics concerns the density of In adatoms. The original (Au, In)/Si(111) surface contains ~ 0.15 ML of In adatoms. With increasing In coverage by 0.2 ML, the hopping rate of single vacancies in the C₆₀ layer decreases by more than an order of magnitude. This finding can be generalized to the conclusion that in complex molecular–atomic systems fine structural features (e.g., changing density of atomic component) can affect greatly the dynamics of vacancies in the molecular layer.

Acknowledgments

This work was supported by the Russian Science Foundation (project No. 14-12-00482). We thank O.A. Utas for the help in processing experimental data.

Appendix A. Supplementary data

Supplementary data to this article can be found online at <http://dx.doi.org/10.1016/j.susc.2015.02.010>.

References

- [1] T. Sakurai, X.-D. Wang, Q. Xue, Y. Hasegawa, T. Hashizume, H. Shinohara, *Prog. Surf. Sci.* 51 (1996) 263.
- [2] P.J. Moriarty, *Surf. Sci. Rep.* 65 (2010) 175.
- [3] P. Moriarty, Y.R. Ma, M.D. Upward, P.H. Beton, *Surf. Sci.* 407 (1998) 27.
- [4] D.L. Keeling, M.J. Humphry, R.H.J. Fawcett, P.H. Beton, C. Hobbs, L. Kantorovich, *Phys. Rev. Lett.* 94 (2005) 146104.
- [5] N. Martsinovich, L. Kantorovich, *Nanotech.* 19 (2008) 235702.
- [6] N. Martsinovich, L. Kantorovich, *Phys. Rev. B* 77 (2008) 115429.
- [7] N. Martsinovich, L. Kantorovich, *Nanotech.* 20 (2009) 135706.
- [8] A. Stróżecka, J. Mysliveček, B. Voigtländer, *Appl. Phys. A* 87 (2007) 475.
- [9] J.A. Larsson, S.D. Elliott, J.C. Greer, J. Repp, G. Meyer, R. Allenspach, *Phys. Rev. B* 77 (2008) 115434.
- [10] M.T. Cuberes, R.R. Schlittler, J.K. Gimzewski, *Appl. Phys. Lett.* 69 (1996) 3016.
- [11] S.H. Chang, I.S. Hwang, C.K. Fang, T.T. Tsong, *Phys. Rev. B* 77 (2008) 155421.
- [12] N. Néel, L. Limot, J. Kröger, R. Berndt, *Phys. Rev. B* 77 (2008) 125431.
- [13] G. Schulze, K.J. Franke, A. Gagliardi, G. Romano, C.S. Lin, A.L. Rosa, T.A. Niehaus, T. Frauenheim, A. Di Carlo, A. Pecchia, J.I. Pascual, *Phys. Rev. Lett.* 100 (2008) 136801.
- [14] G. Schulze, K.J. Franke, J.I. Pascual, *New J. Phys.* 10 (2008) 065005.
- [15] D.A. Olyanich, V.G. Kotlyar, T.V. Utas, A.V. Zotov, A.A. Saranin, *Nanotech.* 24 (2013) 055302.
- [16] See Supplemental Material for STM and simulation movies.
- [17] A. Mayne, F. Rose, C. Bolis, G. Dujardin, *Surf. Sci.* 486 (2001) 226.
- [18] I. Brihuega, O. Custance, J. Gómez-Rodríguez, *Phys. Rev. B* 70 (2004) 165410.
- [19] T. Nagao, S. Hasegawa, K. Tsuchie, S. Ino, C. Voges, G. Klos, H. Pfnür, M. Henzler, *Phys. Rev. B* 57 (1998) 10100.
- [20] D.V. Gruznev, I.N. Filippov, D.A. Olyanich, D.N. Chubenko, I.A. Kuyanov, A.A. Saranin, A.V. Zotov, V.G. Lifshits, *Phys. Rev. B* 73 (2006) 115335.
- [21] J.K. Kim, K.S. Kim, J.L. McChesney, E. Rotenberg, H.N. Hwang, C.C. Hwang, H.W. Yeom, *Phys. Rev. B* 80 (2009) 075312.
- [22] A.V. Matetskiy, D.V. Gruznev, A.V. Zotov, A.A. Saranin, *Phys. Rev. B* 83 (2011) 195421.
- [23] D.V. Gruznev, A.V. Matetskiy, L.V. Bondarenko, O.A. Utas, A.V. Zotov, A.A. Saranin, J.P. Chou, C.M. Wei, M.Y. Lai, Y.L. Wang, *Nat. Commun.* 4 (2013) 1679.
- [24] A.V. Matetskiy, L.V. Bondarenko, D.V. Gruznev, A.V. Zotov, A.A. Saranin, J.P. Chou, C.R. Hsing, C.M. Wei, Y.L. Wang, *Surf. Sci.* 616 (2013) 44.
- [25] N.V. Sibirev, V.G. Dubrovskii, A.V. Matetskiy, L.V. Bondarenko, D.V. Gruznev, A.V. Zotov, A.A. Saranin, *Appl. Surf. Sci.* 307 (2014) 46.